

Monolithically integrated multi-wavelength VCSEL arrays using high-contrast gratings

Vadim Karagodsky¹, Bala Pesala¹, Christopher Chase¹, Werner Hofmann¹,
Fumio Koyama² and Connie J. Chang-Hasnain^{1,*}

¹Department of Electrical Engineering and Computer Science, University of California at Berkeley,
Cory Hall, CA, Berkeley, 94720, USA

²Tokyo Institute of Technology 4259-R2-22, Nagatsuta, Midoriku, Yokohama 226-8503, Japan
[*cch@eecs.berkeley.edu](mailto:cch@eecs.berkeley.edu)

Abstract: We propose a novel design for multi-wavelength arrays of vertical cavity surface-emitting lasers (VCSELs) using high-contrast gratings (HCGs) as top mirrors. A range of VCSEL cavity wavelengths in excess of 100 nm is predicted by modifying only the period and duty-cycle of the high-contrast gratings, while leaving the epitaxial layer thickness unchanged. VCSEL arrays fabricated with this novel design can easily accommodate the entire Er-doped fiber amplifier bandwidth with emission wavelengths defined solely by lithography with no restrictions in physical layout. Further, the entire process is identical to that of solitary VCSELs, facilitating cost-effective manufacturing.

©2010 Optical Society of America

OCIS codes: (050.2770) Gratings; (250.7260) Vertical cavity surface emitting lasers; (140.2010) Diode laser arrays.

References and links

1. C. Chang-Hasnain, M. Maeda, N. Stoffel, J. Harbison, L. Florez, and J. Jewell, "Surface Emitting Laser Arrays with Uniformly Separated Wavelengths," *Electron. Lett.* **26**(13), 940–941 (1990).
2. C. Chang-Hasnain, J. Harbison, C. Zah, M. Maeda, L. Florez, N. Stoffel, and T. P. Lee, "Multiple Wavelength Tunable Surface Emitting Laser Arrays," *IEEE J. Quantum Electron.* **27**(6), 1368–1376 (1991).
3. L. Eng, K. Bacher, W. Yuen, J. Harris, Jr., and C. Chang-Hasnain, "Multiple Wavelength Vertical Cavity Laser Arrays on Patterned Substrates," *IEEE J. Quantum Electron.* **1**(2), 624–628 (1995).
4. F. Koyama, T. Mukaiyama, Y. Hayashi, N. Ohnoki, N. Hatori, and K. Iga, "Wavelength control of vertical cavity surface-emitting lasers by using nonplanar MOCVD," *IEEE Photon. Technol. Lett.* **7**(1), 10–12 (1995).
5. T. Wipiejewski, M. Peters, E. Hegblom, and L. Coldren, "Vertical-cavity surface-emitting laser diodes with post-growth wavelength adjustment," *IEEE Photon. Technol. Lett.* **7**(7), 727–729 (1995).
6. C. F. R. Mateus, M. C. Y. Huang, Y. Deng, A. R. Neureuther, and C. J. Chang-Hasnain, "Ultrabroadband mirror using low-index cladded subwavelength grating," *IEEE Photon. Technol. Lett.* **16**(2), 518–520 (2004).
7. M. Huang, Y. Zhou, and C. Chang-Hasnain, "A surface-emitting laser incorporating a high-index-contrast subwavelength grating," *Nat. Photonics* **1**(2), 119–122 (2007).
8. C. Chang-Hasnain, Y. Zhou, M. Huang, and C. Chase, "High-Contrast Grating VCSELs," *IEEE J. Sel. Top. Quantum Electron.* **15**, 869–878 (2009).
9. Y. Zhou, M. Moewe, J. Kern, M. C. Huang, and C. J. Chang-Hasnain, "Surface-normal emission of a high-Q resonator using a subwavelength high-contrast grating," *Opt. Express* **16**(22), 17282–17287 (2008).
10. Y. Zhou, V. Karagodsky, B. Pesala, F. G. Sedgwick, and C. J. Chang-Hasnain, "A novel ultra-low loss hollow-core waveguide using subwavelength high-contrast gratings," *Opt. Express* **17**(3), 1508–1517 (2009).
11. V. Karagodsky, M. C. Y. Huang, and C. J. Chang-Hasnain, "Analytical Solution and Design Guideline for Highly Reflective Subwavelength Gratings," in *Proceedings of Conference on Lasers and Electro-Optics (CLEO'08)*, San Jose, USA, Paper number JTUA128, (2008).
12. M. G. Moharam, and T. K. Gaylord, "Rigorous coupled-wave analysis of planar-grating diffraction," *J. Opt. Soc. Am.* **71**(7), 811–818 (1981).
13. W. Hofmann, E. Wong, G. Böhm, M. Ortsiefer, N. H. Zhu, and M. C. Amann, "1.55 μm VCSEL Arrays for High-Bandwidth WDM-PONs," *IEEE Photon. Technol. Lett.* **20**(4), 291–293 (2008).
14. A. Yariv, *Optical Electronics in Modern Communications*, (Oxford University Press, 1997)

1. Introduction

The increasing demands of high bandwidth applications, such as online video streaming or real-time video conferencing, have been a major driving force for high capacity data networks. In addition, high speed optical interconnects operating at bandwidths greater than 1 Tb/s are attractive compared to electrical interconnects due to their low power consumption and compact size. Wavelength division multiplexing (WDM) offers an ideal way to leverage the high bandwidth of an optical fiber ($\gg 1$ Tb/s) while using existing electronics operating close to 10 Gb/s. Consequently, monolithically-integrated, low cost, high-speed, multi-wavelength (MW) sources are extremely desirable. Surface normal emission, wafer scale manufacturing and testing makes vertical-cavity surface-emitting lasers (VCSELs) a cost effective solution for MW sources [1,2]. MW VCSEL sources can also be cost effective solutions for a wide range of applications including optical trace-gas sensing, displays, etc.

All monolithically integrated MW VCSEL arrays fabricated to date utilize thickness variations either in the distributed Bragg reflector (DBR) or cavity layers to achieve different emission wavelengths [1,2]. A change in the layer thickness directly translates to a change in the lasing wavelength due to the round trip phase condition of a VCSEL cavity [1,2]. Thickness variations achieved by leveraging the natural non-uniformity in a molecular beam epitaxy (MBE) system [1,2], patterned substrates [3], nonplanar metalorganic chemical vapor deposition [4], or anodic oxidation of a GaAs spacer layer [5] were reported. However, none of the previously reported techniques led to precise control of the lasing wavelength. In addition, due to complicated fabrication processes, these techniques are not readily scalable to a large number of VCSEL arrays.

In this work, we propose a novel method of fabricating MW VCSEL arrays with an unprecedented wavelength range by simply varying the lateral dimensions of high-contrast gratings (HCGs), lithographically defined on the same single layer. This novel design is based on our prior works on HCG, a single layer grating providing reflectivity at least as high as 40 pairs of epitaxially grown DBRs [6–8]. Note that our previously reported HCG-VCSELs were designed to exhibit large tolerances to grating dimension variations [8]. Yet, with a different design, the phase (but not magnitude) of HCG reflectivity can exhibit a large dependence on dimensions, leading to a wide range of VCSEL emission wavelengths, as reported here for the first time. We show HCG-VCSELs whose wavelengths are significantly varied by tuning grating period and duty cycle (ratio between grating width and period), while keeping the same epitaxy design (same layer thickness), thus enabling the fabrication of MW VCSELs array using simple lithographic means. As the laser wavelength is determined entirely by lithography, this design facilitates precise wavelength control and arbitrary physical layout. In addition, the proposed technique dramatically simplifies the fabrication process, introducing no modification to a typical HCG-VCSEL process flow.

2. The origin of HCG reflectivity

A HCG is comprised of dielectric or semiconductor bars having a high refractive index *fully* surrounded by a low refractive index medium, such as air or SiO₂, with high refractive index contrast between the two media (Fig. 1). The lateral periodicity of the HCG (Λ) must be below the wavelength of the incident wave, otherwise the incident light could be diffracted into higher diffraction orders. Ultra high HCG reflectivity has been reported by our group in broadband [6–8] and resonant narrow-band [9] regimes. High reflectivity can be achieved by design for any incidence angle, starting from surface normal up to grazing incidence angles of less than 1° [10].

The physical mechanism behind the HCG reflectivity is destructive interference [11]. As depicted schematically in Fig. 1, when a wave is incident on the grating, it excites a number of HCG eigenmodes, which propagate towards the bottom grating interface with different phase velocities.

For a well-chosen HCG design, the optical path lengths of these modes can be matched in such a way that the modes (including their reflections) interfere destructively at the bottom grating interface. Destructive interference in this case does not mean that the fields are zero everywhere. Rather, it means that the spatial mode-overlap along the bottom interface with the transmitted plain-wave is zero, yielding a zero transmission coefficient. This prevents optical power from being launched into a transmissive propagating wave, and thus causes full reflection.

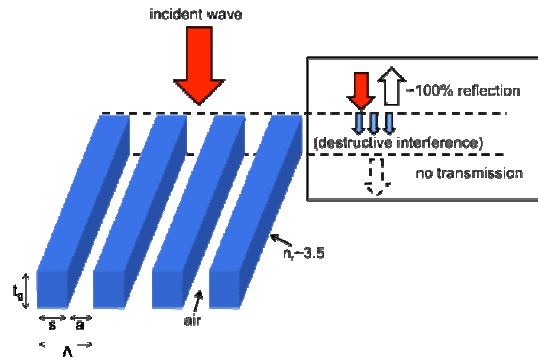


Fig. 1. Schematic of the HCG and its high-reflectivity mechanism. The blue bars represent a semiconductor material with high refractive index of e.g. ~ 3.5 . The grating bars are surrounded by a low index medium, such as air or oxide [6]. When a wave is incident on the grating, its energy is coupled into several eigenmodes of the HCG. These modes propagate through the grating at different phase velocities. For certain HCG designs, the excited set of modes (including their reflections) interferes destructively at the bottom grating interface, resulting in zero coupling into a transmitted plane wave, and thus $\sim 100\%$ reflection.

The most significant distinction of HCG from distributed Bragg reflectors (DBRs) or photonic crystal is that in the latter, the reflectivity results from constructive interference of reflection from *multiple*, distributed layers (interfaces). This and other distinctions lead to several advantages in an HCG, including a small thickness, polarization selectivity and a broad reflection bandwidth [6].

In this manuscript the reflectivity of HCG is simulated using the Rigorous Coupled Wave Analysis (RCWA) [12], which is a broadly accepted method that uses a matrix formalism to analytically solve for the reflected and transmitted diffraction orders of planar gratings. For purposes of verification, our group has also developed our own analytical solution for subwavelength HCGs [11], based on mode matching between the modes inside HCG and the free space modes outside it. Based on numerous comparisons, we have found excellent agreement between RCWA and our mode matching calculations.

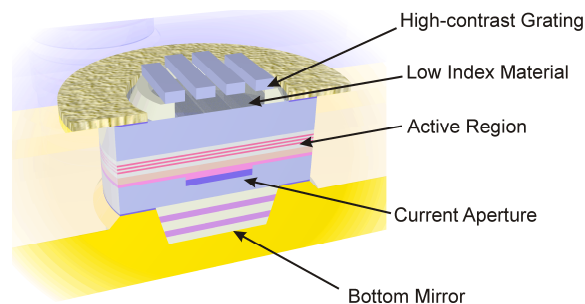


Fig. 2. 1550-nm VCSEL schematic. This device consists of, starting from the bottom, a conventional dielectric DBR as bottom mirror, VCSEL cavity serving as heat and current spreader including an active region and a current aperture, topped by an air gap with an HCG above as top-reflector.

3. HCG VCSEL design

The VCSEL cavity structure used in our simulations is similar to the previously demonstrated high-speed 1550-nm VCSEL designs [13], with the epitaxial top mirror being replaced by a HCG structure. A schematic VCSEL design is shown in Fig. 2. The active region consists of multiple InGaAlAs quantum wells. Current confinement can be achieved by an aperture formed by a buried tunnel junction, placed at the minimum of the optical field [13]. The out-coupling mirror is a HCG, lithographically formed out of a semiconductor material like InP, with an air-gap underneath. In principle, the top two layers could also be designed to be SiO₂ as the low index material and Si as the HCG, as used in [6].

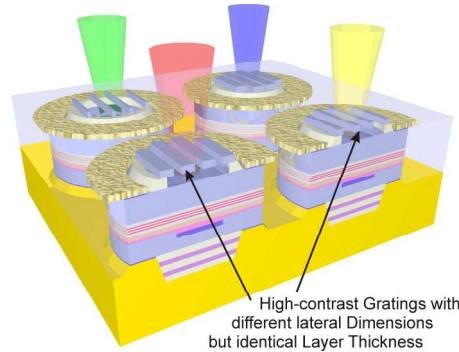


Fig. 3. Schematic of the proposed HCG VCSEL array. Modifying the lateral dimensions of the HCG from VCSEL to VCSEL changes the HCG reflectivity phase, which facilitates control over the lasing wavelength of each VCSEL. Thus, a MW VCSEL array can be created.

4. Multi-wavelength HCG-VCSEL array design

The VCSEL wavelength is determined by the round-trip 2π phase condition (Eq. (1)) as in any Fabry-Perot cavity:

$$4\pi \frac{L_{\text{cavity}}}{\lambda_{\text{Lasing}}} + \phi_{\text{HCG}} + \phi_{\text{DBR}} = 2\pi m, \quad (1)$$

L_{cavity} being the physical length of the cavity, λ_{Lasing} being the lasing wavelength, ϕ_{HCG} and ϕ_{DBR} being the reflectivity phases of the HCG and DBR mirrors, respectively, and m is an integer. Hence, to attain a large wavelength range in λ_{Lasing} with the same epitaxy, i.e. same L_{cavity} (ϕ_{DBR} being relatively insensitive to λ_{Lasing}), we need a design of HCG whose ϕ_{HCG} can be changed greatly with grating period and duty cycle. In this case, by using a *thicker* HCG to facilitate a longer propagation length for the eigenmodes, the destructive interference condition can be achieved (to yield a high reflectivity) with a larger wavelength dependence in phase. This leads to a possibility to significantly change λ_{Lasing} using only moderate changes in HCG lateral dimensions. This design is highly desirable for fabricating post-epitaxy MW VCSEL arrays in a controllable fashion with an especially large wavelength tuning range. A schematic of a MW VCSEL array utilizing this wavelength tuning paradigm is presented in Fig. 3. A reasonable HCG thickness of only 900 nm is already thick enough to provide wavelength tuning range in excess of 100 nm, as presented in Figs. 4 and 5.

Figure 4 shows how using two HCGs with different lateral dimensions but an otherwise identical VCSEL structure results in satisfying the round trip 2π phase condition in Eq. (1) at two different wavelengths (1450 nm and 1550 nm), while maintaining the HCG reflectivity well above 99.9% at the lasing wavelengths, which is also necessary for achieving a high Q cavity with low mirror losses [14].

In some VCSEL designs, reflectivity of 99.9% might be too high for light extraction. In those cases, we can just as easily design the reflectivity to be slightly less (e.g. ~99.5%).

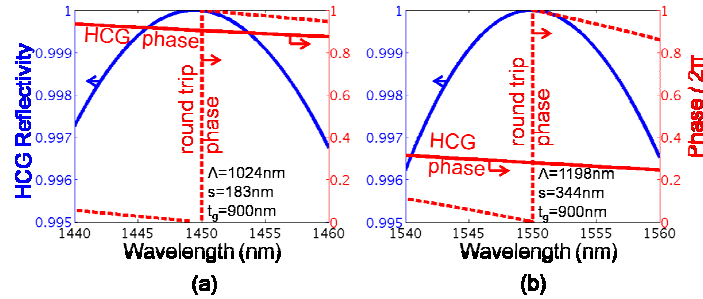


Fig. 4. Example of two HCG mirror designs facilitating lasing at two different wavelengths: 1450 nm (a) and 1550 nm (b). The HCG thickness is identical in both designs, since all HCGs are patterned on the same layer. The lateral dimensions (HCG period, Λ , and bar width, s) are varied. Thicker HCGs can facilitate larger potential phase shift. An HCG thickness of 900 nm provides considerable change in HCG phase with small change in lateral dimensions. This results in a wide variation of lasing wavelengths. High quality factor is achieved by high reflectivities (>99.5%) of HCG and DBR mirrors.

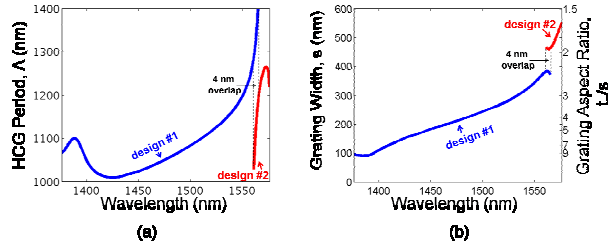


Fig. 5. Span of HCG lateral dimensions, i.e. HCG period (a) and HCG bar width (b), which satisfies lasing conditions across a 200 nm wavelength tuning range, ending at 1576 nm. The design comprises of two parts: the first ending at 1565 nm and the second beginning at 1561 nm, leaving a 4 nm overlap. Each wavelength within the tuning range has at least one suitable HCG design. The relatively small grating aspect ratios shown in (b) are well within the fabrication capabilities of common lithography techniques.

By optimizing the lateral HCG dimensions for additional wavelengths, we have found a collection of dimensions suitable for lasing at every wavelength between 1376 nm and 1576 nm, all with the same HCG thickness of 900 nm. These optimized HCG dimensions are presented in Figs. 5(a), 5(b) (blue and red curves) as a function of lasing wavelength, demonstrating expected wavelength tuning range in excess of 100nm. All these dimensions satisfy the phase condition in Eq. (1) and correspond to very high HCG reflectivity (>99.9%). The difference between the blue and red curves (designs #1 and #2) in Fig. 5 is the integer m in Eq. (1). Figure 5 shows that for some wavelengths, more than one choice of HCG dimensions will facilitate lasing. In the case of Fig. 5 there is a 4nm wavelength window, at which two different HCG designs are suitable for lasing. This overlap window between two different HCG designs is necessary to make sure that the wavelength tuning range is continuous, i.e. without wavelength gaps, at which no design works. This way, when one of the designs can no longer be pushed to higher wavelengths, we can switch to a second HCG design (with different dimensions) and extend the tuning range even further. It is possible that further optimization will reveal that in some VCSEL structures, a chain of three and more HCG designs will provide an even larger tuning range. In order to make the HCG design in Fig. 5 easily fabricatable, special attention was paid during the optimization process to only use HCG dimensions which are well within the specs of current lithography techniques, as indicated by the relatively small grating aspect ratios shown in Fig. 5b.

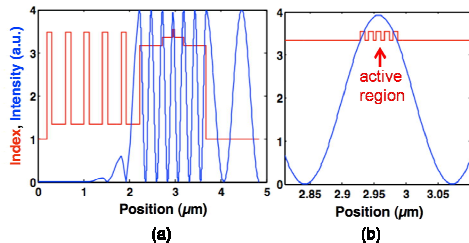


Fig. 6. (a) Field intensity profile (blue) of the cavity of a MW HCG VCSEL structure overlaid on refractive index of the materials (red) at 1570 nm. (b) Field profile of the active region.

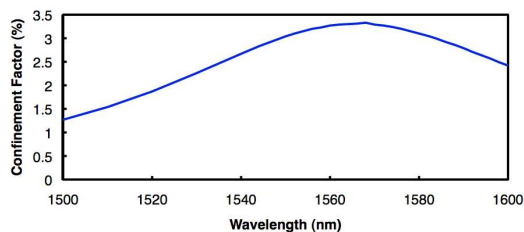


Fig. 7. Confinement factor of the HCG MW VCSEL array as a function of wavelength. Over the 32 nm of the range (1550-1582 nm), the confinement factor is still >90% of its peak value.

5. Cavity simulation

In order to verify the influence of the HCG phase tuning on the standing cavity wave and the confinement factor of the VCSEL, transfer matrix calculations were performed. Figure 6 shows the standing cavity wave (blue) at 1570 nm with the index profile (red) overlaid for comparison, demonstrating a good overlap of the quantum wells with the field in the optical cavity. The confinement factor was estimated for various wavelengths from 1500 to 1600 nm and is presented in Fig. 7. It was calculated by integrating the field in the active region and dividing by the integral of the total field in the VCSEL structure (excluding the HCG). The lateral confinement was estimated to be 1. Over an optical bandwidth of 32 nm, corresponding to the bandwidth of the entire C-band, the so-called “erbium-window”, the confinement factor is still >90% of its peak value, indicating that all C-band wavelengths could be addressed by variation of lateral HCG dimensions, while keeping fairly uniform device performance. Since the HCG dimensions in Fig. 5 and the confinement factors in Fig. 7 show robust performance of the proposed structure across a very large wavelength range, the bottleneck that will ultimately determine the tuning range will be the gain bandwidth of the active region.

6. Conclusion

We present a novel design for a multi-wavelength HCG VCSEL array, whereby the wavelength range is obtained by only varying the lateral dimensions of the HCG, while the layer thickness remains constant for all devices, in order to facilitate fabrication flow compatible with epitaxy. This enables wavelength tuning mechanism based solely on lithography, facilitating a very simple fabrication flow. The predicted cavity wavelength range approaches 200 nm. We believe the HCG-VCSEL reported here would enable a new type of cost-effective WDM source suitable to accommodate the full bandwidth of Er-doped fiber amplifier. The same concept may be applied to fabricate multi-wavelength filter and detector arrays.

Acknowledgements

We wish to acknowledge the support of a National Security Science and Engineering Faculty Fellowship and the National Science Foundation CIAN NSF ERC grant #EEC-0812072.